Design and Fabrication of An Integrated CMOS-MEMS 3-Axis Accelerometer

Huikai Xie[1,*], Gary K. Fedder[1,2], Zhiyu Pan[3], Wilhelm Frey[3]

[1]Department of Electrical and Computer Engineering and [2]The Robotics Institute, Carnegie Mellon University, Pittsburgh, PA 15213, USA
[3]Research and Technology Center, Robert Bosch Corporation, 4009 Miranda Ave, Palo Alto, CA 94304
[*]Now at Department of Electrical and Computer Engineering, University of Florida, Gainesville, FL 32611, USA

ABSTRACT

A monolithic integrated CMOS-MEMS three-axis accelerometer has been designed and fabricated. The sensor is a single structure that uses sidewall capacitors of comb fingers to sense acceleration in all three directions. The sensor plus on-chip CMOS circuitry is about 1mm by 1mm in size and is fabricated by a post-CMOS micromachining process that uses interconnect metal layers as etching mask and has only dry-etch steps involved. The sensor structure incorporates both thin-film structures and bulk Si structures to achieve three-axis acceleration sensing without any extra masks, material deposition or wafer bonding. Both behavioral simulaton and finite element simulation were conducted to verify and optimize the sensor design. A noise floor of 50 $\mu g/Hz^{1/2}$ can be achieved.

Keywords: Integrated accelerometer, 3-axis accelerometer, CMOS-MEMS, vertical comb finger sensing

1 INTRODUCTION

Miniature three-axis accelerometers are often required in automobiles, navigation systems and some medical applications such as monitoring rehabilitation training for hemiplegic patients [1]. However, most of existing micromachined accelerometers are uni-axial or dual-axial. In general, bulk micromachining is suitable for making z-axis accelerometers with capacitive parallel plates or piezoresistive beams. Surface micromachining, on the other hand, can be used to fabricate lateral-axis accelerometers with capacitive interdigitated comb fingers. By assembling and orienting orthogonally two or three accelerometers, tri-axial acceleration sensing can be obtained, but the package size and cost will be dramatically increased.

Various 3-axis accelerometers have been reported [2-6]. Among them, bulk micromachined 3-axis accelerometers normally have large mass but require wafer bonding, wet etching and two-side alignment. Surface micromachined tri-axial accelerometers have integrated interface circuitry but small mass. Lemkin *et al* demonstrated a surface micromachined integrated 3-axis accelerometer [2]. Kruglick *et al* made a piezoresistive 3-axis accelerometer using conventional CMOS processing followed by a xenon difluoride Si release etch [3]. Acceleration detection parallel to the chip plane is implemented by lifting out of plane two accelerometers with aluminum hinges. Toda *et al* [4] reported a spherical 3-axis accelerometer based on Ball Semiconductor Technology [5]. The proof mass, which is 1mm in diameter and weighs 1.2 milligram, is electrostatically levitated without mechanical suspension.

In this paper, the authors proposed and fabricated a monolithic 3-axis accelerometer design based on a deep reactive-ion-etch (DRIE) CMOS-MEMS process [7]. In this new design, a single microstructure senses all three-axis accelerations and is integrated with interface circuits on a single CMOS chip. Large proof mass is obtained by using silicon substrate as the structural material.

2 DRIE CMOS-MEMS

The process flow is shown in Fig. 1. The CMOS chip is etched from its back side, leaving a 10 μm to 100 μm-thick

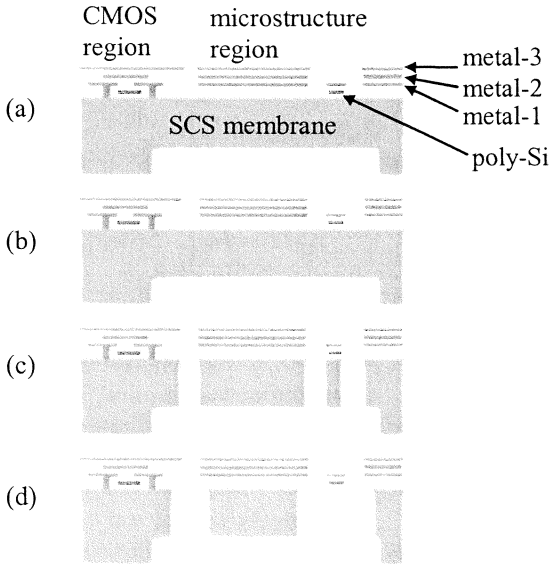

Figure 1. Cross-sectional view of the DRIE CMOS-MEMS process. (a) Backside etch. (b) Oxide etch. (c) Deep Si etch. (d) Si undercut.

single-crystalline silicon (SCS) membrane (Fig. 1(a)). This backside deep Si etch step is used to control the thickness of microstructures. Next, an anisotropic dielectric etch is performed from the front side using the top metal layers as etching mask (Fig. 1(b)). Then, another deep Si etch is used to release microstructures (Fig. 1(c)). The last isotropic Si etch step (Fig. 1(d)) provides a specific undercut of bulk Si to create compliant structures along with thick, stiff Si structures.

3 ACCELEROMETER DESIGN

3.1 Three-Axis Motion Sensing

The principle of lateral-axis and z-axis capacitive comb finger sensing is illustrated in Fig. 2. If the metal layers on the stators and rotors are electrically connected, respectively, the CMOS comb drive functions just like a lateral-axis polysilicon comb drive (Fig. 2(a)). If all three metal layers in the stators are electrically connected while the metal-1 and metal-3 in the rotors are separately connected, two sidewall capacitors, C_1 and C_2, are formed, as shown in Fig. 2(b). When the rotor moves due to an external acceleration, C_1 and C_2 will change values in opposite directions. Because of the high wiring flexibility, a fully differential capacitive bridge can be easily formed. Such a z-axis accelerometer in a thin-film CMOS-MEMS process was previously demonstrated [8].

All the comb fingers have a "T" shape cross-section due to the silicon undercut. As shown in Fig. 3, electrodes are only placed at the sidewall edges to reduce the parasitic capacitance overlap to the silicon layer. The parasitics can be further reduced by using narrower silicon layer. The width of the silicon layer is controlled by the silicon undercut (see Fig. 1(d)). The silicon layer should not be too narrow (~2 μm), as the mechanical robustness over manufacturing variations must be maintained.

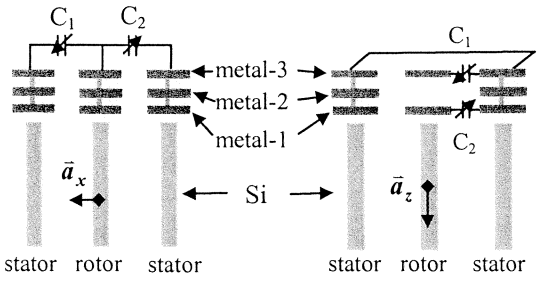

Figure 2. Three-dimensional sensing.
(a) Lateral sensing; and (b) vertical sensing.

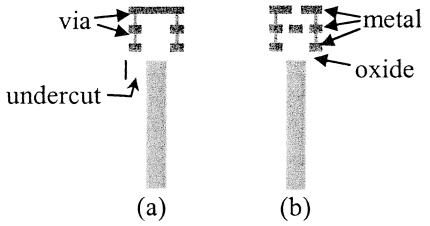

Figure 3. Comb finger configuration with reduced parasitics. (a) Single electrode. (b) Two separate electrodes.

3.2 Spring Designs

A z-axis compliant spring is shown in Fig. 4(a), which is realized by connecting multiple beams with short trusses and using beams with metal-2 or metal-3 on the top. Beams with metal-1 on the top are even more compliant in the z-direction, but they have large out-of-plane curling. Narrow beams are used in the spring to guarantee the complete undercut of silicon to form a z-compliant thin-film structure. The multiple beams with short trusses can increase the stiffness in the lateral direction to reduce cross-axis sensitivity.

The x/y-axis spring is obtained by symmetrically arranging four sub-springs as shown in Fig. 4(b). Each sub-spring consists of rectangularly closed beams in series which are flexible in both the x and y directions. Xie *et al* used a similar flexure in a gyroscope design [8]. The advantage of this x/y-axis spring is that the stiffness coefficients in the x and y directions are equal.

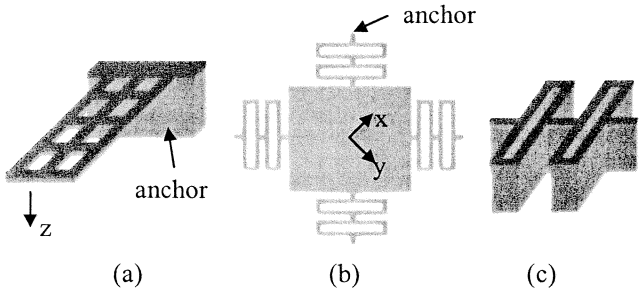

Figure 4. Spring designs. (a) z-axis spring; (b) top view of the x-y springs with a central plate; and (c) Side view of one x-y spring branch.

3.3 Topology Design

The topology of the 3-axis accelerometer is shown in Fig. 5. The comb fingers for x-axis sensing form eight capacitors, i.e., four C_{i1}'s and four C_{i2}'s where i = 1,2,3,4. Let $C_i = C_{i1} + C_{i2}$. Because of the symmetry, the C_i's are insensitive to y-axis acceleration to first order. C_1 and C_2

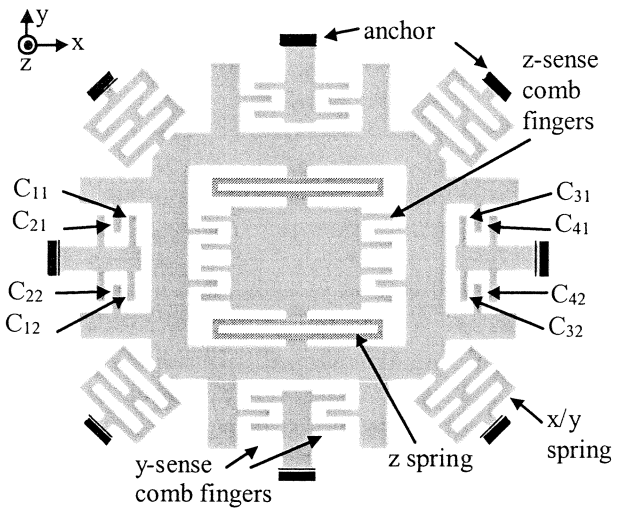

Figure 5. Topology of the 3-axis accelerometer.

form a differential capacitive divider, and so do C_3 and C_4. Thus, a full differential capacitive bridge is obtained using the four C_i's. As there is silicon underneath the spring beams, the springs are much stiffer (about two orders of magnitude) in the z-direction than in the x- or y-direction, which significantly reduces the z-axis cross-sensitivity. The same rationale applies to the y-axis acceleration sensing.

The z-axis acceleration sensing is obtained by embedding a z-axis accelerometer in the center of the whole structure. The suspension of the z-axis accelerometer is in the form of the flexure shown in Fig. 4(a), which is flexible in the z-direction. Again, the cross-axis acceleration contributions are rejected by the differential capacitive topology. It should be noted that the differential capacitors in the z-axis accelerometer are stacked vertically (as shown in Fig. 2(b)) and separated into groups.

4 STRUCTURAL SIMULATION

NODAS (Nodal Design of Actuators and Sensors) is a hierarchical cell library for behavioral modeling and nodal simulation of MEMS [10]. It consists of symbols and models of elements commonly found in suspended MEMS designs, such as anchors, beams, plates and gaps. As shown in Fig. 2, the cross-section of the DRIE beams is not rectangular. A DRIE beam has a wider CMOS layer on top of the silicon layer. This irregular cross section has been considered and adopted in the DRIE beam models in the NODAS library.

Fig. 6(a) shows the NODAS model for an x-y accelerometer. The plate represents the proof mass. Each x-y spring consists of a group of beams. Note that the model was rotated 45° compared to Fig. 5. The simulation results are plotted in Fig. 6(b). Table 1 lists the design parameters of the 3-axis accelerometer. The symmetry of the x/y springs gives the same first resonance (4.8 kHz) for both x- and y- axes. A torsional force was also applied with respect to the y-axis, which gives a 6.3 kHz torsional mode. The z-stiffness in the x/y springs is much larger because of the thick silicon layer. A 15.9 kHz resonance along the z-axis was obtained from the simulation. A similar NODAS model was used for the embedded z-axis accelerometer, in which the z-axis resonance is 4.2 kHz.

Table 1. Design parameters of the 3-axis accelerometer

	X	Y	Z
Proof mass (μg)	73	73	40
Resonance (kHz)	4.8	4.8	4.2

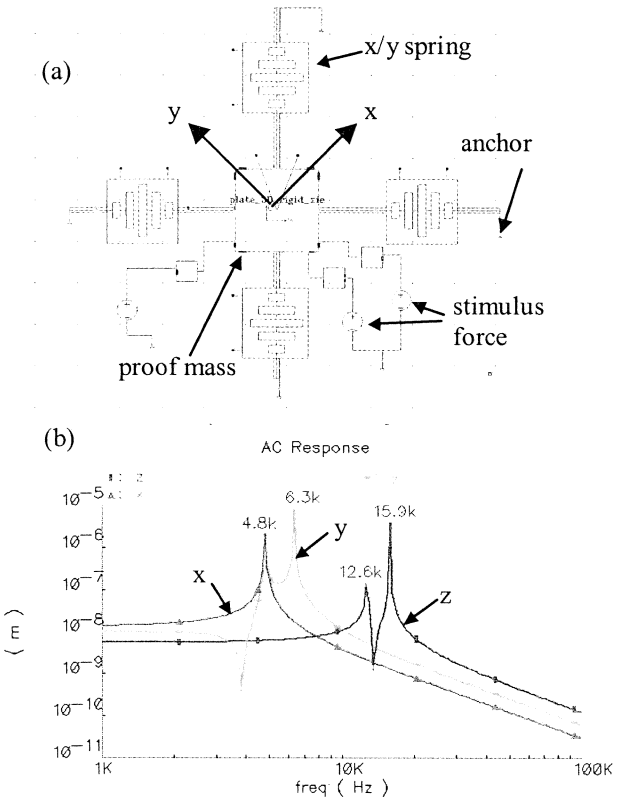

Figure 6. Behavioral simulation of the x/y-axis accelerometer. (a) NODAS model. (b) NODAS simulation result.

5 FABRICATION RESULTS

A released device is shown in Fig. 7, in which the x- and y- accelerometers are identical and orthogonally oriented, while the z-accelerometer is embedded in the center. The microstructure is about 1mm by 1mm in size. The silicon layer is about 60μm thick. The final silicon undercut step is very critical. Silicon underneath the z-

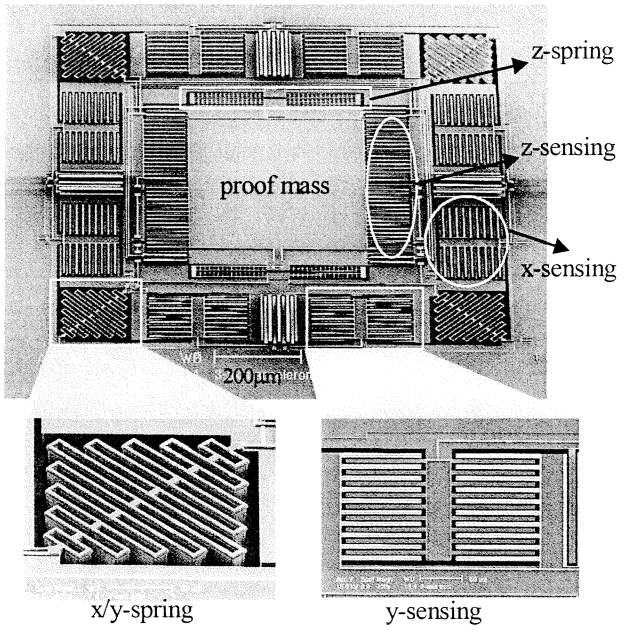

Figure 7. Micrographs of a released 3-axis accelerometer.

spring beams was completely undercut to maximize the z-compliance. Silicon underneath the x/y-spring beams was just partially undercut to maintain the flatness of the whole structure. The silicon undercut on the comb fingers with

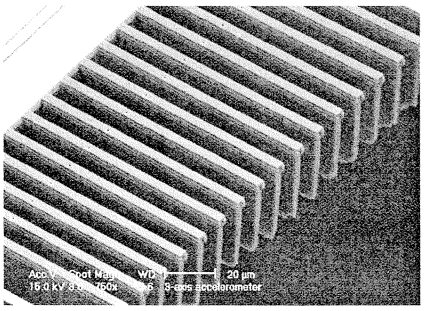

Figure 8. SEM of comb fingers

small gaps was significantly reduced because of the loading effect. A SEM of comb fingers with one side stripped off is shown in Fig. 8.

6 CONCLUSION

A monolithic, integrated 3-axis accelerometer was designed and fabricated. Its compact size and potential low cost make it attractive to health care applications and consumer electronics. Its high resolution and on-chip signal processing capability are also suitable for space and automobile industries.

ACKNOWLEDGEMENT

This research effort was partially sponsored by DARPA and the U.S. AFRL, under agreement number F30602-99-2-0545.

REFERENCES:

[1] Y. Higashi *et al*, "Monitoring rehabilitation training for hemiplegic patients by using a tri-axial accelerometer," Engineering in Medicine and Biology Society, 2001. Proceedings of the 23rd Annual International Conference of the IEEE, Vol.2 (2001), pp. 1472- 1474.

[2] M. Lemkin and B.E. Boser, "A three-axis micromachined accelerometer with a CMOS position-sense interface and digital offset-trim electronics," IEEE Journal of Solid-State Circuits, Vol. 34 (1999), no. 4 , pp. 456 -468.

[3] E. Kruglick, B. Warneke, and K. Pister, " CMOS 3-axis accelerometers with integrated amplifier," MEMS'98, Heidelberg, Germany, Jan. 1998, pp. 631-636.

[4] R. Toda, N. Takeda, T. Murakoshi, S. Nakamura and M. Esashi, "Electrostatically levitated spherical 3-axis accelerometer," Proceedings of MEMS 2002, Las Vegas, NV, USA (Jan. 2002), pp. 710-713.

[5] N. Takeda, "Ball Semiconductor Technology and Its Application to MEMS," Proceedings of MEMS 2000, Miyazaki, Japan (Jan. 2000), pp. 23-27.

[6] H. Takao, H. Fukumoto, and M. Ishida, "A CMOS integrated three-axis accelerometer fabricated with commercial submicrometer CMOS technology and bulk-micromachining," *IEEE Transactions on Electron Devices*, Vol. 48 (2001), pp. 1961 -1968.

[7] H. Xie, L. Erdmann, X. Zhu, K.J. Gabriel, G.K. Fedder, "Post-CMOS processing for high-aspect-ratio integrated silicon microstructures," Journal of Microelectromechanical Systems, Vol. 11 (2001), no.2, pp. 93 -101.

[8] H. Xie and G.K. Fedder, "Vertical Comb-finger Capacitive Actuation and Sensing for CMOS-MEMS," Sensors & Actuators: A, Vol. 95 (2002), pp. 212-221.

[9] S.S. Baek, Y.S. Oh, B.J. Ha, S.D. An, B.H. An, H. Song, C.M. Song, "A symmetrical z-axis gyroscope with a high aspect ratio using simple and new process,", 1999.. Twelfth IEEE International Conference on Micro Electro Mechanical Systems (MEMS '99), pp. 612 -617.

[10] Q. Jing and G.K. Fedder, "A hierarchical circuit-level design methodology for microelectromechanical systems," IEEE Transactions on Circuits and Systems II, Vol. 46 (1999).